IMPACT OF MgCl₂ ADDITION ON THE FORMATION OF NANO-CRYSTALLINE HERCYNITE SYNTHESISED BY CO-PRECIPITATION METHOD

ALI BAGHAEI*, #SASAN OTROJ**, SAEID BAGHSHAHI*, M. MASOUD MOHEBI*

*Department of Materials Science and Engineering, Faculty of Engineering,
Imam Khomeini International University, Qazvin, Iran
**Faculty of Engineering, Shahrekord University, Shahrekord, Iran

#E-mail: sasan.otroj@gmail.com

In this paper, the effect of MgCl₂ addition on the synthesis of hercynite was investigated. For this reason, hercynite was prepared by co-precipitation of AlCl₃·6H₂O and FeCl₂·4H₂O along with various amounts of MgCl₂ at 60°C. Then, the co-precipitated materials were calcined at 1300, 1400 and 1500 °C in air atmosphere. Afterwards, phase composition and microstructure of samples were studied by X-ray diffraction (XRD) analysis and scanning electron microscopy (SEM). The results showed that the formation of hercynite simply took place with the presence of MgCl₂ due to the release of Mg²⁺ cations and then, the formation of spinel structure and its evolution to hercynite structure. Moreover, the addition of MgCl₂ influences the amount of hercynite phase. Calcination temperature affects hercynite crystallite sizes so that hercynite crystallite sizes increas by the increasing of calcination temperature from 1300°C to 1500°C.

INTRODUCTION

$FeAl_2O_4$ is a mixed oxide normal spinel that belongs to the isometric crystal system of the hexoctahedral class. In this system, one eighth of the tetrahedral sites are occupied by Fe^{2+} cations and one half of the octahedral sites are occupied by Al^{3+} cations. Sometimes, depending on the synthesis process, the Fe^{2+} cations can also occupy octahedral sites [1, 2]. In nature, iron aluminate $FeAl_2O_4$ (hercynite) is rarely encountered and is abundant in rocks with a high degree of metamorphism. It forms associations with andulasite $Al_2[SiO_4]O$, sillimanite $Al(AlSiO_5)$, and garnet $Fe_3Al_2Si_3O_{12}$ (almandine) [3]. There are many reports which introduced hercynite as a chromium-free substitute for magnesia-chrome bricks for the burning zone of rotary kilns. To synthesise hercynite, FeO needs to react with Al_2O_3 in its stable form with the proper temperature and partial pressure of oxygen (pO_2); otherwise, the synthesis of hercynite will fail. Recently, Chen et al. [1] synthesised hercynite by a reaction sintering method using industrial alumina, mill scale ($FeO + Fe_2O_3$), and carbon black as starting materials in the presence of nitrogen and solid carbon at high temperatures. Dutta et al. [2] synthesised nano-crystalline $FeAl_2O_4$ from the heating of iron and aluminium acetylacetonate complexes and studied the magnetic property of the $FeAl_2O_4$ nano-particles. Hercynite was synthesised in an Ar atmosphere by thermal treatment of mechano-chemically activated metal Al and Fe_3O_4 as starting materials; however, Fe, magnetite, or haematite remained in the final product [4]. In another

report, it was synthesised with $\lambda = 8.140$ Å under a shock wave acting with axisymmetric loading on gibbsite $Al(OH)_3$ placed in a steel storage ampul. It was formed, evidently, as a result of the interaction under high pressure and temperature of the products of decomposition of aluminium hydroxide with the steel wall of the ampul [3]. It was reported that radial combustion experiments were conducted on Fe_2O_3/aluminium thermite thin circular samples. In fact, a stoichiometric ($Fe_2O_3 + 2Al$) and four over aluminized mixtures were tested. The main products were identified as alumina (α-Al_2O_3) and iron (Fe). Meanwhile, a significant amount of hercynite ($FeAl_2O_4$) was detected, decreasing with the aluminium excess in the reactants [5]. Andreozzi et al. [6] synthesised a new blue hercynite-based pigment, stable at the processing temperatures for the ceramic application by thermal treatment of commercial α-alumina, $(NH_4)_2TiO(SO_4)_2$, and $(NH_4)_2Fe(SO_4)_2$ in Ar/4 % H_2 atmosphere. Mukhopadhyay et al. [7] developed novel Al_2O_3-$FeAl_2O_4$ nano-composites by precipitation of $FeAl_2O_4$ particles through reduction aging of Al_2O_3-10 wt. % Fe_2O_3 solid solutions in N_2/4 % H_2. It has been demonstrated that reduction of the dissolved Fe^{3+} in the Al_2O_3-Fe_2O_3 solid solutions to Fe^{2+} during aging in the reducing atmosphere results in the precipitation of Fe^{2+}-containing second phase particles ($FeAl_2O_4$) due to the low solubility of Fe^{2+} in Al_2O_3 [7, 8]. The object of the present work is to investigate the effect of $MgCl_2$ on the synthesis of hercynite via co-precipitation method. For this reason, the aluminium chloride hexahydrate and iron (II) chloride tetrahydrate were used as raw

materials with various amounts of $MgCl_2$ for preparing the hercynite. Then, the co-precipitated materials were calcined at 1300, 1400 and 1500°C under air atmosphere. The diffractometric technique and scanning electron microscopy were used to investigate the produced materials in this study.

EXPERIMENTAL

Mixed solution of stoichiometric aluminium chloride hexahydrate and iron (II) chloride tetrahydrate (Merck, Germany) with $Fe^{2+}:Al^{3+}$ ratio of approximately 1:2 were prepared by dissolving the corresponding amounts of aluminium chloride hexahydrate and iron (II) chloride tetrahydrate in distilled water at 60°C. Then, different molar ratios (0.125 to 1) of magnesium chloride (Merck, Germany) were added to the primary solution. After mixing the corresponding chlorides, these solutions were stirred with excess of NaOH (Merck, Germany) solution at pH 9.5 – 10.5. The gelatinous precipitates were kept at 60°C for 1 h, cooled to room temperature, rinsed for several times by distilled water until free from chloride ions as well as produced NaCl and finally dried at 110°C for 24 h. Then, dried powders were calcined at 1300, 1400 and 1500°C for 5 h. Phase composition of calcined powders were characterised by X-ray diffraction (XRD) analysis (Bruker, D8 advance, Germany) using Cu Kα radiation (λ = 1.5406 Å) equipped with DIFFRAC^{plus} software for data acquisition, handling and determining the proportion of hercynite phase in compositions by semi-quantitative XRD analysis. This analysis was performed on the base of patterns relative heights and of their I/I_{cor} values (I: intensity of certain amount of every crystalline phase; I_{cor}: intensity of certain amount of corundum phase). In fact, the software made a comparison between phases intensities and their I/I_{cor} data on PDF database to calculate the approximately concentration of phases. Moreover, this calculation is based on a hypothesis that all phases are crystalline and detected. Microstructure of

calcined powders was examined by scanning electron microscopy (SEM; VEGA, TESCAN, Czech Republic) equipped with energy dispersive spectroscopy (EDS; SAMx, France).

RESULTS

Phase composition of calcined powders

XRD results of prepared samples containing different $MgCl_2$ molar ratios after calcination at 1300°C are shown in Figure 1.

With respect to these results, haematite (Fe_2O_3) and corundum (Al_2O_3) phases are found in the composition without $MgCl_2$; in fact, no hercynite phase was formed in this composition. Generally, the amorphous aluminium and iron hydroxides were dehydrated into Al_2O_3 and Fe_2O_3 by the increase of temperature. It can be seen that the hercynite phase was formed in compositions by the addition of Mg^{2+} resulting from dissolved $MgCl_2$. Furthermore, hercynite phase contents in the composition were enhanced with the increasing of $MgCl_2$, showing that hercynite phase content affected by changing the amount of $MgCl_2$. The broadened diffraction peaks in the XRD results of the calcined samples indicate the small grains size and poor crystallinity of the hercynite phase. The XRD results of prepared samples containing different molar ratios of $MgCl_2$ after heating at 1400°C are shown in Figure 2.

As it can be seen from the results of Figure 2, changes in the composition of phases with increasing $MgCl_2$ content are similar to the results of Figure 1. The amount of hercynite, indeed, was increased by the increase of $MgCl_2$ content in the composition. In addition, it can be seen that the specimen containing 1 molar ratio of $MgCl_2$ mainly exhibits the existence of single phase hercynite, and no impurity peaks are observed which indicates the starting materials have fully reacted. Drawing a comparison between Figure 1 and Figure 2, reveals that the intensity of the diffraction peaks of the
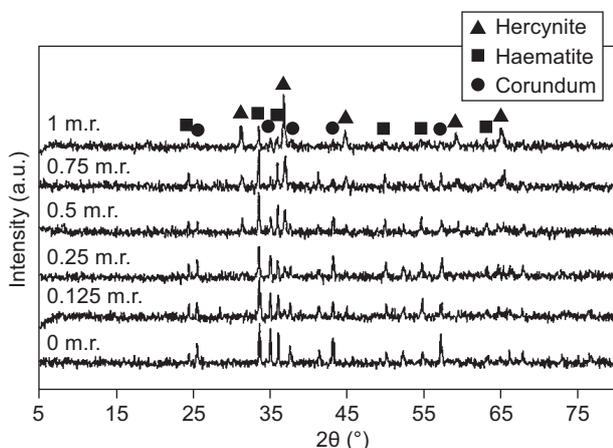
Figure 1. XRD results of the specimens containing different molar ratios of $MgCl_2$ calcined at 1300°C.
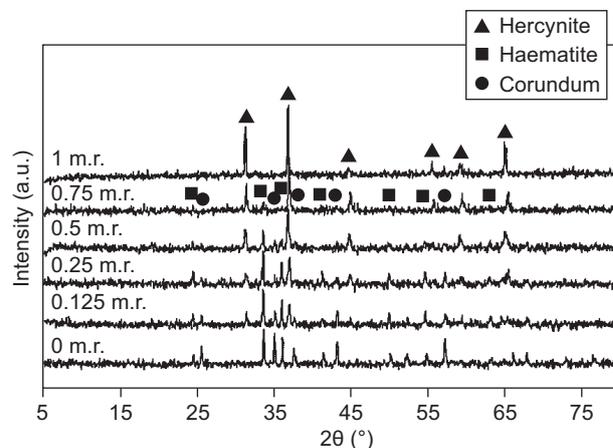
Figure 2. XRD results of the specimens containing different molar ratios of $MgCl_2$ calcined at 1400°C.

hercynite phase gradually increases by the increase of calcination temperature to 1400°C, and the diffraction peaks of the hercynite become stronger and sharper after calcination at 1400°C. Sharp diffraction peaks in the XRD results of the calcined samples at 1400°C indicate larger crystallite size and higher crystallinity of the hercynite phase in comparison with calcined samples at 1300°C. Therefore, one can see that crystallite size of hercynite depends on the calcination temperature. The XRD results of calcined samples at 1500ºC are shown in Figure 3.
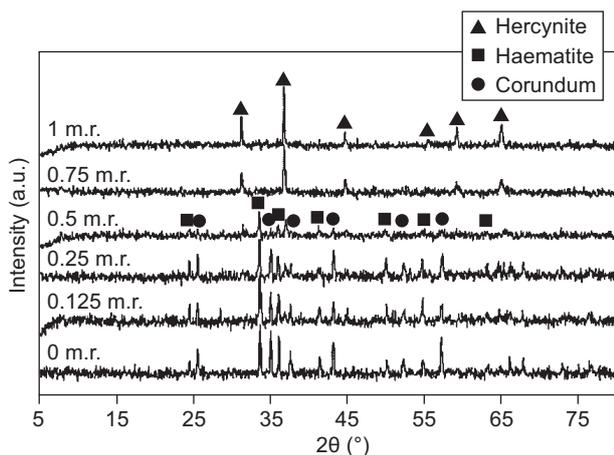
Figure 3. XRD results of the specimens containing different molar ratios of $MgCl_2$ calcined at 1500°C.

As it has been shown, the specimen without $MgCl_2$ contained of haematite and corundum. In fact, hercynite was not formed in air atmosphere by the increase of temperature to 1500°C. Hercynite phase was formed in calcined samples at 1500°C by the addition of $MgCl_2$ to compositions similar to samples which, were calcined at 1300°C and 1400°C. In addition, changes in phase composition were similar to results of Figure 1 and Figure 2, and formed hercynite phase was increase by the increase of added $MgCl_2$. Specimens with 0.125, 0.25 and 0.5 molar ratios of $MgCl_2$ contained of haematite, corundum and hercynite, and the intensity of hercynite diffraction picks was increased by the increase of $MgCl_2$ ratio while the intensity of haematite and corundum diffraction picks was decreased. Hercynite was the only phase in both compositions containing 0.75 and 1 molar ratios of $MgCl_2$, and no impurity peaks was observed, evidencing that raw materials have fully reacted. Moreover, the diffraction peaks intensity of specimen containing 1 molar ratio of $MgCl_2$ was more than that of the specimen containing 0.75 molar ratio of $MgCl_2$, indicating better crystallinity and larger crystallite sizes. In general, hercynite is synthesised under inert gas or reduction atmosphere [1-4]. By contrast, the results have shown that hercynite can be prepared in air atmosphere by using the co-precipitation method and low cost chemical materials.
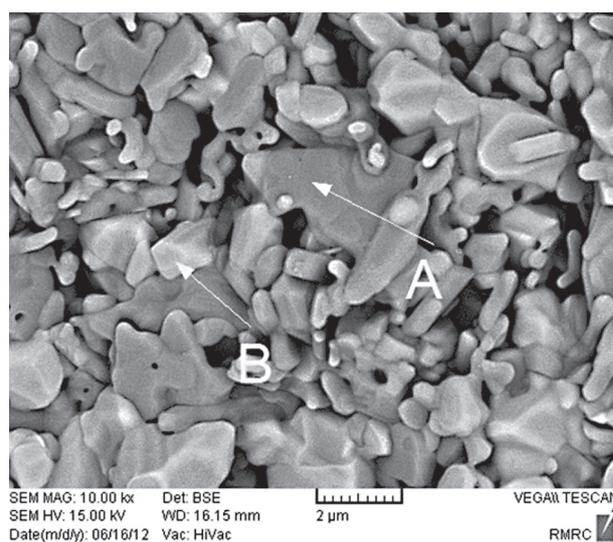
a) 0
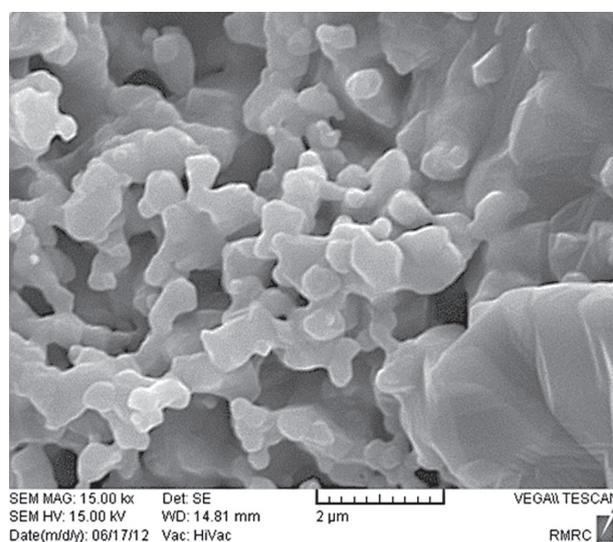
b) 0.5
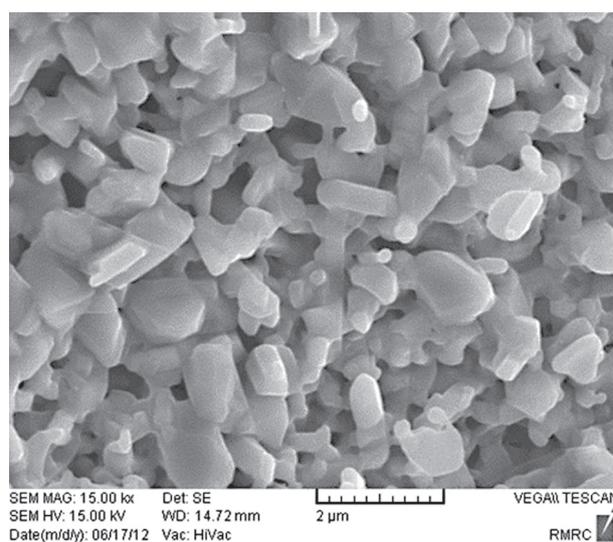
c) 1

Figure 4. SEM micrograph of samples containing different molar ratios of $MgCl_2$; a) 0, b) 0.5 and c) 1, calcined at 1300°C.

Morphology of the calcined powders

The SEM micrographs of calcined samples at 1300°C containing different molar ratios of $MgCl_2$ are shown in Figure 4a-c.

As shown, the composition without $MgCl_2$ contains the crystalline phases which have hexagonal and spherical form. According to the EDS analyses (Figure 5a and 5b.), the grey hexagonal particles were corundum whereas the white spherical particles were haematite.

The average particle size significantly decreases with the addition of $MgCl_2$ and then, tends to increase by further addition of $MgCl_2$. Moreover, it was found that many ultra-fine octahedral or cubic particles were formed when the $MgCl_2$ was introduced into composition. The nano-crystalline hercynite appeared at all calcination temperatures. Figure 6 demonstrates the microstructures of calcined samples at 1400°C containing different molar ratios of $MgCl_2$.

With microstructural evaluation, one can see that the addition of $MgCl_2$ leads to the formation of higher octahedral hercynite in the composition after calcination at 1400°C. Meanwhile, the grain size of formed hercynite

a) 0

b) 0.5

a)

b)

c) 1
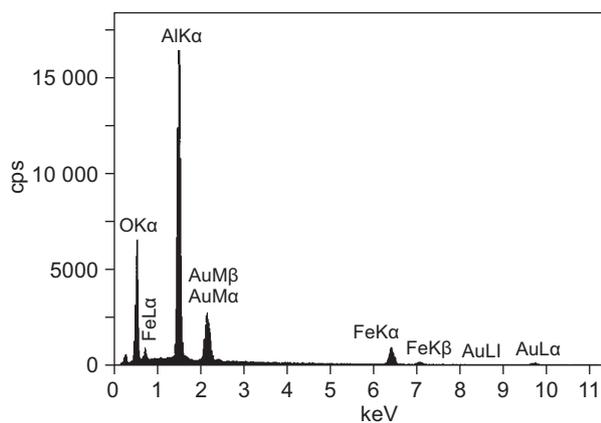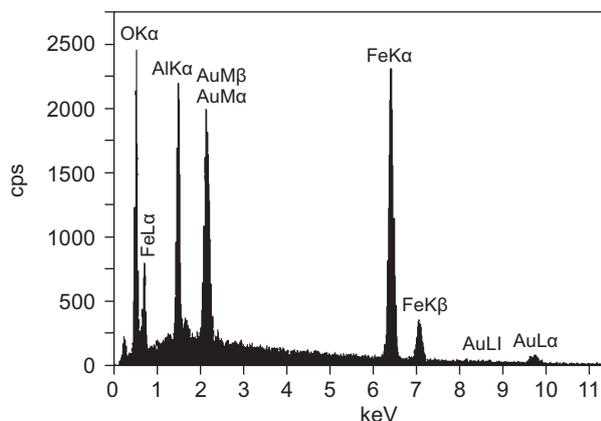
Figure 5.   EDS pattern of gray (a) and white (b) particles showed in Figure 4a.
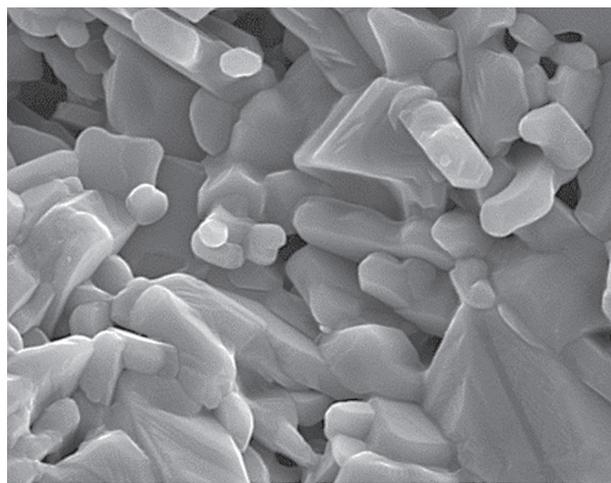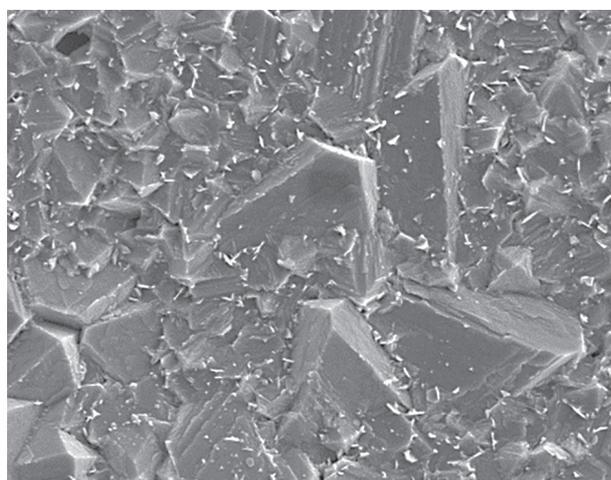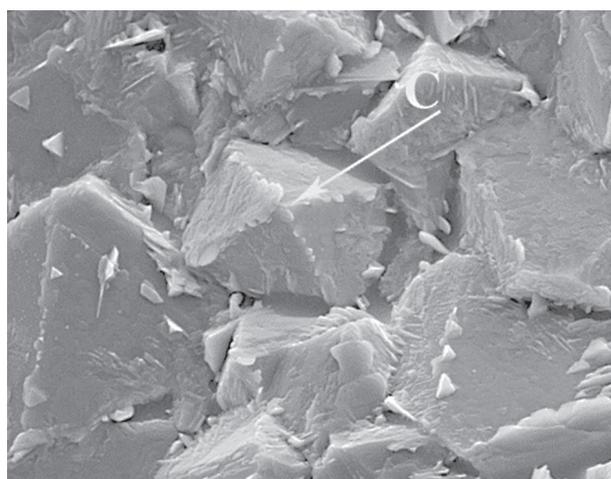
Figure 6.   SEM micrograph of samples containing different molar ratios of MgCl₂; a) 0,) 0.5 and c) 1, calcined at 1400°C.

significantly increases by the addition of $MgCl_2$ which can be clearly seen in SEM micrographs. The well-crystallised hercynite crystals connected with each other, indicating that the synthesised hercynite using this method was of high purity [1].

According to the EDS analysis (Figure 7), the octahedral particles contained both Mg and Fe, which confirms the formation of a solid solution based on $Fe(Mg)O \cdot Al_2O_3$.
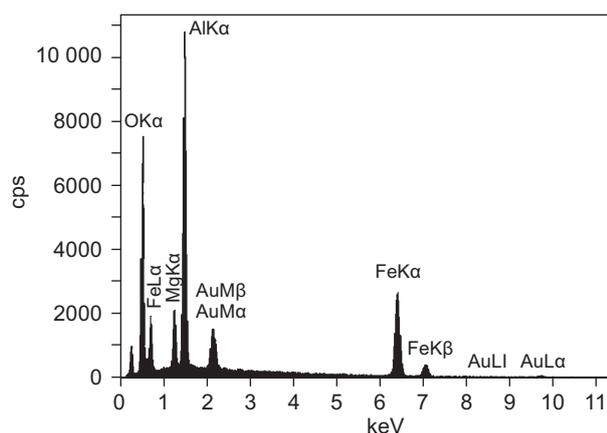
Figure 7. EDS pattern of octahedral particle (C) showed in Figure 6c.

By making a comparison between microstructures of calcined samples at 1300 and 1400°C, one can see that the calcination temperature caused a drastic change in particles size and morphology of hercynite. Hence, the exaggerated grain growth is observed and the sintering process is occurred in calcined samples at 1400°C. Thus, well-crystallised grains of hercynite were formed at 1400°C and the homogeneous microstructure is obtained.

Microstructures of calcined samples at 1500°C containing different molar ratios of $MgCl_2$ are shown in Figure 8a-c. It can be seen that the grain size of sample without $MgCl_2$ additive was large enough to be considered as exaggerated grain growth. This can be considered as the corresponding crystal structures of haematite and corundum and high calcination temperature. Sintering process was happened in all samples and the grain sizes of samples were decreased by the increasing of $MgCl_2$ addition. Besides, the sample containing 1 molar ratio of $MgCl_2$ had a particulate microstructure in which grains were deformed due to high calcination temperature and shape of corners and edges has been changed.

Drawing a comparison between Figures 6 and 8 revealed that grain sizes of hercynite decreased in samples containing more $MgCl_2$ content by increasing calcination temperature from 1400°C to 1500°C. This phenomenon could be because of more grain growth rate at 1400°C, for this temperature was optimum sintering temperature, and grain growth rate decreased by increasing the calcination temperature to 1500°C and passing the optimum sintering temperature.
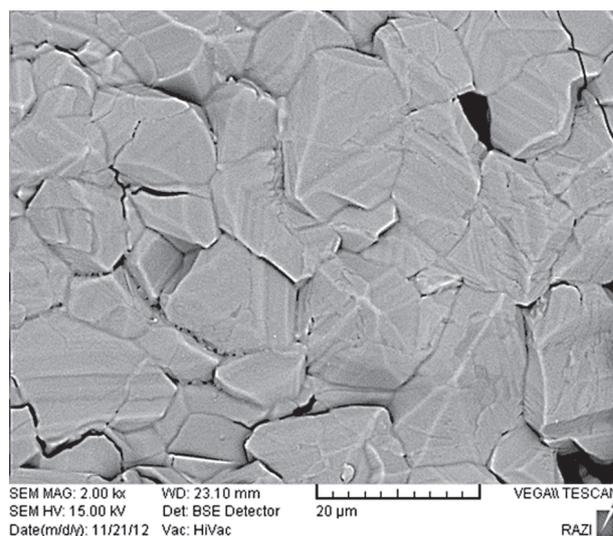
a) 0
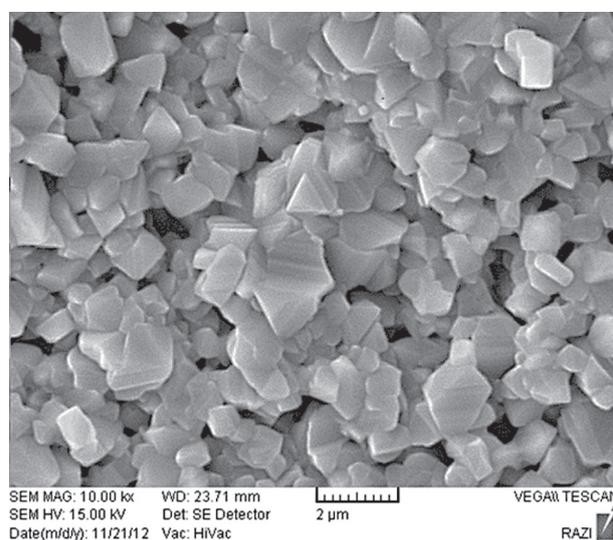
b) 0.5
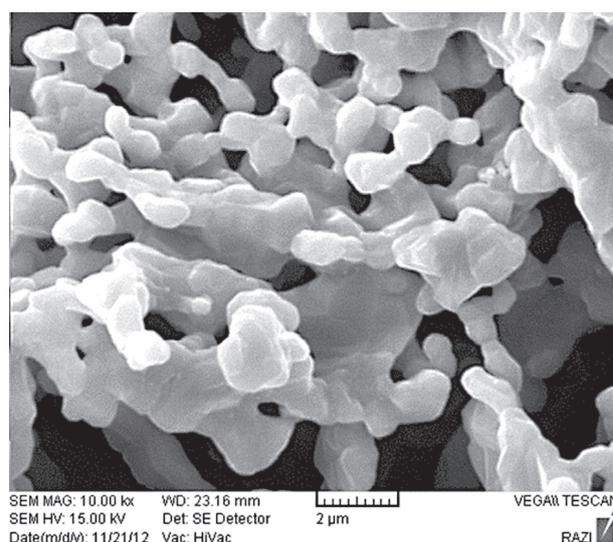
c) 1

Figure 8. SEM micrograph of samples containing different molar ratios of $MgCl_2$; a) 0, b) 0.5 and c) 1, calcined at 1500°C.

DISCUSSION

The proportion of formed hercynite in compositions was determined by semi-quantitative XRD analysis. The results are shown in Figure 9 as a function of used $MgCl_2$ molar ratio in the composition and calcination temperature.
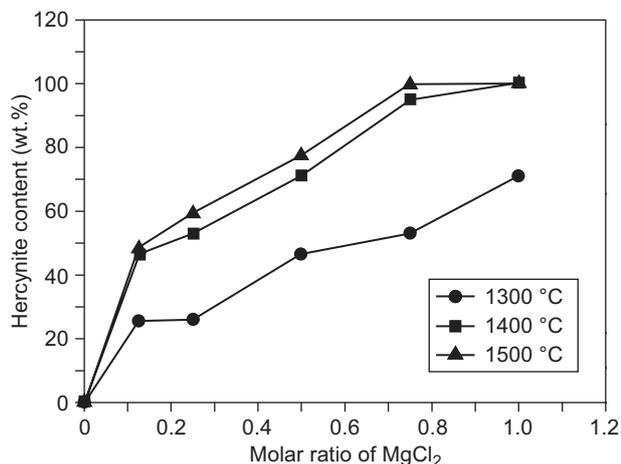
Figure 9. The effect of $MgCl_2$ molar ratio on the formed hercynite as a function of calcination temperature.

With respect to these results, the hercynite phase was formed simply in the presence of $MgCl_2$ and its content was enhanced by the increase of $MgCl_2$ molar ratio. Therefore, it can be concluded that the amount of formed hercynite in the final composition depends on $MgCl_2$ molar ratio in raw materials composition. Hercynite phase was formed completely in the composition containing 1 molar ratio of $MgCl_2$ after calcination at 1400°C and in both composition containing 1 and 0.75 molar ratios of $MgCl_2$ after calcination at 1500°C. Therefore, the temperature of 1400°C and 1500°C are favourable for the formation of hercynite by this method. The observed behaviour would be related to the formation of spinel ($MgAl_2O_4$) in the composition with the addition of $MgCl_2$. In this way, the spinel phase forms at lower temperatures and then, reacts with haematite by the increase of temperature. In addition, spinel is a ternary oxide that its chemical formula is AB_2O_4, where A represent a divalent metal cation which, normally occupies a tetrahedral site and B represents trivalent metal cations that normally occupy the octahedral sites of a cubic packed crystal [9, 10]. The reaction between spinel and haematite leads to the formation of hercynite. Generally, the Fe^{3+} changes into Fe^{2+} with increasing of temperature; afterwards, Fe^{2+} dissolves in the spinel structure in the course of calcination which leads to the formation of $(Fe,Mg)Al_2O_4$ hercynite by the evolution of spinel into hercynite.

The crystallite size of hercynite was determined by measuring the full width at half maximum (FWHM) of the peak at $d = 0.244$ nm, using the Scherrer equation.

The relation between crystallite size of formed hercynite and $MgCl_2$ molar ratio as a function of calcination temperature is shown in Figure 10.
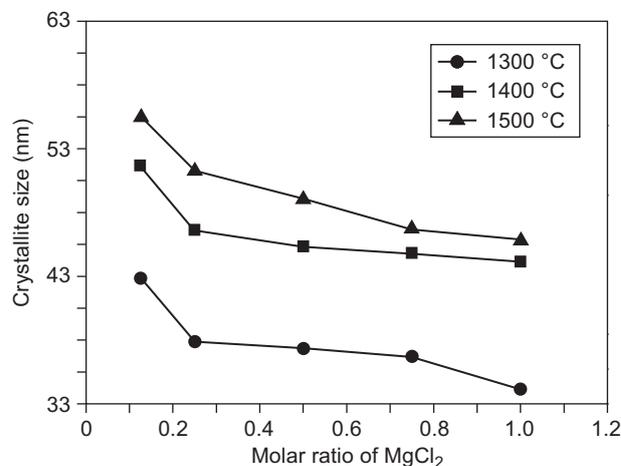
Figure 10. The effect of $MgCl_2$ molar ratio on the crystallite size of hercynite as a function of calcination temperature.

The hercynite crystallite size is increased noticeably by the increase of calcination temperature as shown in Figure 10. Meanwhile, the hercynite crystallite size is decreased with the addition of $MgCl_2$. In fact, it can be regarded as smaller Mg^{2+} cation radius in comparison with Fe^{2+} cation radius.

CONCLUSIONS

The effect of $MgCl_2$ on the synthesis of hercynite via co-precipitation method was investigated. The present method suggests an interesting alternative for the preparation of hercynite with homogeneous microstructure which can be obtained in air atmosphere. In fact, the results showed that hercynite can be formed with the presence of $MgCl_2$. Moreover, the addition of $MgCl_2$ influences the amount of hercynite phase. The amount of hercynite, indeed, is enhanced by the increase of $MgCl_2$ content which can be due to the release of Mg^{2+} cations; then, the formation of spinel structure with the addition of $MgCl_2$. Besides, the calcination temperature affects hercynite crystallite sizes so that hercynite crystallite sizes increas by the increasing of calcination temperature from 1300°C to 1500°C.

REFERENCES

1. Chen J., Yu L., Sun J., Li Y., Xue W. : J. Eur. Ceram. Soc. *31*, 259 (2011).
2. Dutta D.P., Sharma G.: Mater. Sci. Eng. B. *176*, 177 (2011).
3. Tsvigunov A.N., Apolenis A.V., Annikov V.É., Raikova V.M.: Glass. Ceram. *64*,11 (2007).

4. Botta P.M., Aglietti E.F., Porto López J.M.: Mater. Chem. Phys. *76*, 104 (2002).
5. Durães L., Costa B.F.O., Santos R., Correia A., Campos J., Portugal A.: Mater. Sci. Eng. A. *465*, 199 (2007).
6. Andreozzi G.B., Baldi G., Bernardini G.P., Benedetto F.D., Romanelli M.: J. Eur. Ceram. Soc. 24, 821 (2004).
7. Mukhopadhyay A., Todd R.I.: J. Eur. Ceram. Soc. *30*, 2905 (2010).
8. Mukhopadhyay A., Todd R.I.: J. Eur. Ceram. Soc. *31*, 339 (2011).
9. Zawrah M.F., Hamaad H., Meky S.: Ceram. Int. *33*, 969 (2007).
10. Walker E.H., Owens J.W., Etienne M., Walker D.: Mater. Res. Bull. *37*, 1041 (2002).

―――――――